Contents lists available at ScienceDirect

# Biomaterials

# The formulation of aptamer-coated paclitaxel–polylactide nanoconjugates and their targeting to cancer cells

Rong Tong [a], Linda Yala [b], Timothy M. Fan [c], Jianjun Cheng [a,d,e,f,*]

[a] Department of Materials Science and Engineering, University of Illinois at Urbana-Champaign, Urbana, IL 61801, USA
[b] The School of Molecular and Cellular Biology, University of Illinois at Urbana-Champaign, Urbana, IL 61801, USA
[c] Department of Veterinary Clinical Medicine, University of Illinois at Urbana-Champaign, Urbana, IL 61801, USA
[d] Department of Chemistry, University of Illinois at Urbana-Champaign, Urbana, IL 61801, USA
[e] Department of Bioengineering, University of Illinois at Urbana-Champaign, Urbana, IL 61801, USA
[f] Micro- and Nanotechnology Laboratory, University of Illinois at Urbana-Champaign, Urbana, IL 61801, USA

## ARTICLE INFO

## ABSTRACT

Paclitaxel–polylactide (Ptxl–PLA) conjugate nanoparticles, termed as nanoconjugates (NCs), were prepared through Ptxl/(BDI)ZnN(TMS)$_2$ (BDI = 2-((2,6-diisopropylphenyl)-amido)-4-((2,6-diisopropylphenyl)-imino)-2-pentene)-mediated controlled polymerization of lactide (LA) followed by nano-precipitation. Nanoprecipitation of Ptxl–PLA resulted in sub-100 nm NCs with monomodal particle distributions and low polydispersities. The sizes of Ptxl–PLA NCs could be precisely controlled by using appropriate water-miscible solvents and by controlling the concentration of Ptxl–PLA during nano-precipitation. Co-precipitation of a mixture of PLA–PEG–PLA (PLA = 14 kDa; PEG = 5 kDa) and Ptxl–PLA in PBS resulted in NCs that could stay non-aggregated in PBS for an extended period of time. To develop solid formulations of NCs, we evaluated a series of lyoprotectants, aiming to identify candidates that could effectively reduce or eliminate NC aggregation during lyophilization. Albumin was found to be an excellent lyoprotectant for the preparation of NCs in solid form, allowing lyophilized NCs to be readily dispersed in PBS without noticeable aggregates. Aptamer–NCs bioconjugates were prepared and found to be able to effectively target prostate-specific membrane antigen in a cell-specific manner.

## 1. Introduction

Polymeric nanoparticles (NPs) are attractive drug delivery vehicles [1]. They have been employed for the delivery of many types of chemotherapeutic agents for cancer treatment [2–5]. In these polymeric NPs, chemotherapeutic agents are either encapsulated in polymer matrices [6] or covalently conjugated to polymers via hydrolysable or enzymatically degradable linkages. Ideally, systemically administered NPs are able to bypass the recognition of the reticuloendothelial system (RES), extravasate at the leaky tumor vasculatures [3], penetrate and homogeneously distribute in solid tumor tissues [7], get internalized by the target cancer cells, penetrate cellular and subcellular membranes, and then release the payload in the cytoplasma of the target cancer cells in a sustained manner.

NPs that can successfully overcome all these systemic, tissue and cellular barriers are yet to be developed. However, much information has been accumulated in the last 10–20 years for the control of the physicochemical properties of NPs and for the correlation of these properties with the *in vivo* biodistribution and antitumor efficacy of NPs [8]. Although the ideal physicochemical properties of NPs for drug delivery applications have not been completely elucidated, a general consensus about important parameters of NPs, such as particle size, drug loading, loading efficiency, and release kinetics, that are critical to their *in vivo* applications, have been reached [3,4]. The sizes of NPs should typically be controlled at less than 200 nm with narrow polydispersities to give satisfactory *in vivo* biodistribution [3]. High drug loadings, quantitative loading efficiencies and controlled release profiles are also desirable for the *in vivo* applications of NPs [9,10].

Polylactide (PLA), a biodegradable and non-cytotoxic material, has been extensively used in the formulation of particles for biotechnology and drug delivery applications [11–13]. NPs are typically prepared via nanoprecipitation of PLA and drugs [13]. However, this conventional method tends to give NPs with various formulation challenges remaining to be addressed. PLA/drug NPs typically show "burst" drug release profiles in aqueous solution; as much as 80–90% of the encapsulated drug is rapidly released during the first few to

* Corresponding author at: Department of Materials Science and Engineering, University of Illinois at Urbana, Urbana, IL 61801, USA. Tel.: +1 217 244 3924; fax: +1 217 333 2736.
E-mail address: jianjunc@illinois.edu (J. Cheng).

tens of hours [14]. The rapid drug release, also called dose dumping, may cause severe systemic toxicities [1]. In addition, drug loadings in conventional NPs can be very low, typically in a range of 1–5% for most NPs studied [15]. The drug loading of a delivery vehicle has been a critical measure of its utility in clinically settings [15]. At lower drug loadings, larger amounts of delivery vehicles are needed. Because of the limited body weight and blood volume of animals, the administration volumes are usually fixed. For instance, the volume of a solution intravenously administered to mice with 20- to 30-g body weights should be controlled around 100–200 μL [16]. Intravenous administration of NPs with 1% drug loading in a 100-μL solution at a dose of 50 mg/kg to a mouse with 20-g body weight requires the formulation of a concentrated, 1 g/mL NP solution. In practice, it is impossible to formulate such concentrated solutions and inject them intravenously. Furthermore, there is also a lack of general strategy to achieve quantitative drug encapsulation in PLA/drug NPs. Depending on the amount of drug being used, the hydrophobicity and hydrophilicity of drug, and the compatibility of drug and polymer, the encapsulation efficiencies vary drastically in a range of 10–90% [14]. Unencapsulated drugs may self-aggregate [13] and can be very difficult to be removed from the NPs. These formulation challenges significantly impact the processability and the clinical translation of PLA NP delivery vehicles for cancer therapy.

Controlled polymerization methodologies allowing preparations of polyesters [17,18], polypeptides [19,20] and hydrocarbon based synthetic polymers [21] with precisely-controlled molecular weights and narrow polydispersities have been well established. These materials have been extensively utilized in drug delivery. However, controlled polymerization directly used in the formulation of drug delivery vehicles is rare. We recently reported a new method that allows drug molecules to be incorporated into PLA via drug-initiated, controlled ring-opening polymerization of lactide (LA) (Fig. 1 a) [9,10]. Quantitative incorporation of paclitaxel (Ptxl) [9] and other hydroxyl-containing therapeutic molecules [10] have been incorporated to PLA via ester bonds facilitated by Zn-catalysts. When bulky chelating complexes are used, the Zn-catalyst regulates the initiation and polymerization via the least sterically hindered 2′-OH of Ptxl and results in Ptxl–PLA conjugates with precisely controlled composition and molecular weights [9]. At a monomer/initiator (LA/Ptxl) ratio of 10, the drug loading of Ptxl–PLA conjugates and the NPs derived from the conjugates can be as high as 36% with nearly 100% loading efficiencies [9]. Ptxl can be released in a controlled manner with negligible burst from these Ptxl–PLA conjugate NPs, termed nanoconjugates (NCs) to differentiate them from the PLA/drug NPs prepared via encapsulation methods [9].

Extended from these preliminary studies that were mainly focused on controlled polymerization, here we report a comprehensive study of the formulation of Ptxl–PLA NCs as well as the development of cancer targeting NCs by conjugating a cancer-specific targeting aptamer ligand to the surface of NCs. Our study addressed various formulation challenges central to the clinical translation of polymeric NPs, such as control of particle size in salt solution, minimization of NP aggregation during lyophilization and solid formulation, and formulation of NPs in solid form with targeting property well preserved. These techniques may find widespread utility in the controlled formulation of many other polymeric nanomedicines for disease diagnosis, monitoring, and therapy.

## 2. Materials and methods

### 2.1. General

D,L-Lactide (LA) was purchased from TCI America (Portland, OR), recrystallized three times in toluene and stored at −30° C in a glove box prior to use. β-Diimine (BDI) ligand and the corresponding metal complex (BDI)ZnN(TMS)2 were prepared by following the published procedures [17] and stored at −30 °C in a glove box. All

anhydrous solvents were purified by passing the solvents through alumina columns and kept anhydrous by storing them with molecular sieves. Ptxl was purchased from LC Laboratories (Woburn, MA) and stored at −30 °C in a glove box prior to use. All other chemicals were purchased from Sigma–Aldrich (St Louis, MO) and used as received unless otherwise noted. The molecular weights (MWs) of PLA were determined on a gel permeation chromatography (GPC) equipped with an isocratic pump (Model 1100, Agilent Technology, Santa Clara, CA), a DAWN HELEOS 18-angle laser light scattering detector and an Optilab rEX refractive index detector (Wyatt Technology, Santa Barbara, CA). The wavelength of the HELEOS detector was set at 658 nm. Size exclusion columns (Phenogel columns 100 Å, 500 Å, $10^3$ Å and $10^4$ Å, 5 μm, 300 × 7.8 mm, Phenomenex, Torrance, CA) used for the separation of PLA or Ptxl–PLA conjugates were serially connected on the GPC. THF (HPLC grade) was used as the mobile phase of GPC. HPLC analysis was performed on a System Gold system
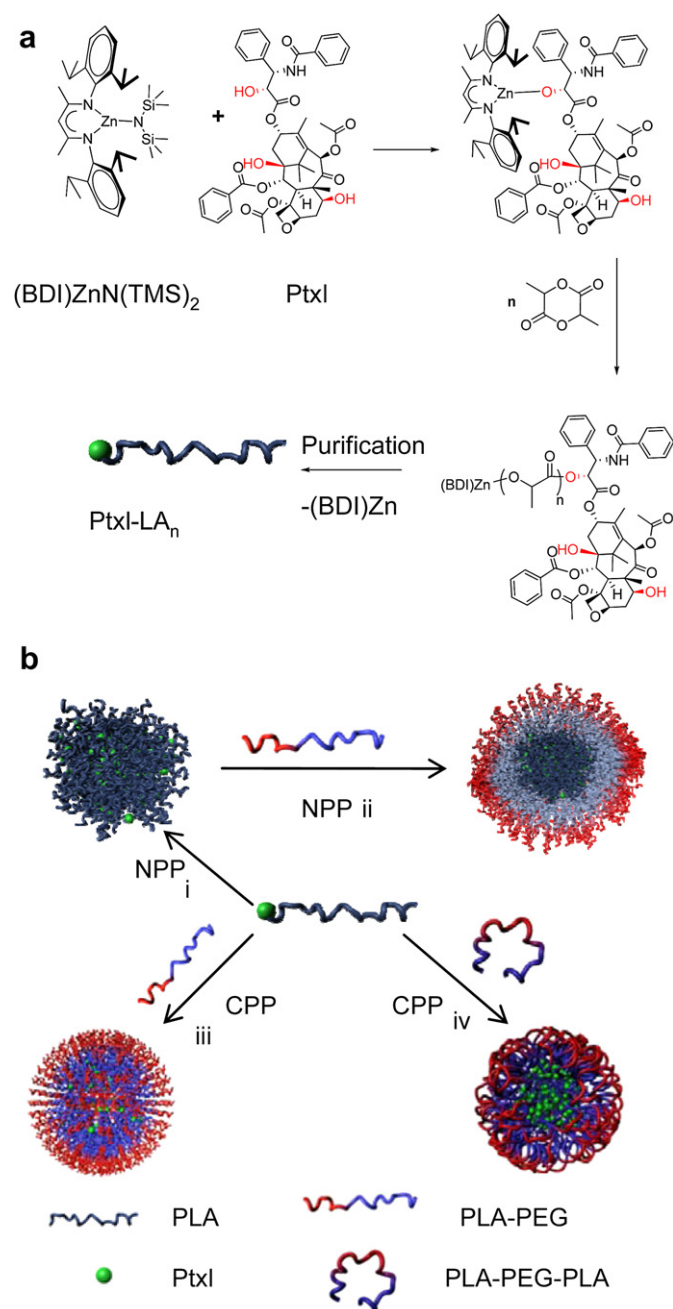


**Fig. 1.** (a) Regioselective initiation and controlled LA polymerization mediated by the Ptxl/(BDI)ZnN(TMS)2 complex to give Ptxl–PLA conjugate. (b) Formulation of Ptxl–PLA NCs through (i) nanoprecipitation of Ptxl–PLA, (ii) nanoprecipitation of Ptxl–PLA followed by coating with PLA–PEG, (iii) co-precipitation of Ptxl–PLA and PLA–PEG, and (iv) co-precipitation of Ptxl–PLA and PLA–PEG–PLA. NPP = nanoprecipitation; CPP = co-precipitation.

(Beckman Coulter, Fullerton, CA) equipped with a 126P solvent module, a System Gold 128 UV detector and an analytical pentafluorophenyl column (Curosil-PFP, $250 \times 4.6$ mm, 5 μ, Phenomenex, Torrance, CA). The UV wavelength for Ptxl analysis was set at 227 nm. The NMR studies were performed on a Varian UI500NB system (500 MHz). The sizes and polydispersities of PLA NCs were determined on a Zeta-PALS dynamic light scattering (DLS) detector (15 mW laser, incident beam = 676 nm, Brookhaven Instruments, Holtsville, NY). The lyophilization of NCs was carried out on a benchtop lyophilizer (Freezone 2.5, Fisher Scientific, Pittsburgh, PA).

## 2.2. Preparation and characterization of Ptxl–LA100

In a glove box, Ptxl (8.5 mg, 0.01 mmol) was dissolved in anhydrous THF (2 mL). (BDI)ZnN(TMS)2 (6.4 mg, 0.01 mmol) was added and allowed to react with Ptxl for 15–20 min. LA (144.0 mg, 1.0 mmol) in THF (1.2 mL) was added dropwise to the vigorously stirred mixture of Ptxl and (BDI)ZnN(TMS)2. The polymerization was monitored using FT-IR by following the disappearance of the lactone band of LA monomer at 1772 cm$^{-1}$ or using $^1$H NMR by checking the methine (–CH–) peak of LA around 5.2–5.0 ppm. After the polymerization was complete, an aliquot of the polymerization solution was analyzed using HPLC to quantify the unreacted Ptxl in order to determine the incorporation efficiency of Ptxl in the Ptxl–PLA conjugates. The resulting Ptxl–PLA conjugate prepared at a LA/Ptxl ratio of 100 (Ptxl–LA100) was precipitated with ethyl ether (10 mL), washed with ether and methanol to remove the BDI ligand, dried under vacuum and characterized by GPC and $^1$H NMR. Complete removal of BDI from Ptxl-PLA conjugate was verified by TLC.

## 2.3. General procedure for the preparation of Ptxl–LA100 NCs via nanoprecipitation

Ptxl–LA100 conjugate in DMF (50 μL, 10 mg/mL) (or in other water-miscible solvent such as acetone) was added dropwise to a nanopure water solution (2 mL). The resulting NCs were analyzed by DLS after nanoprecipitation, collected by ultrafiltration (5 min, 3000× g, Ultracel membrane with 10,000 NMWL, Millipore, Billerica, MA), washed with water to remove DMF (or other organic solvent), and then analyzed by SEM.

## 2.4. Synthesis of PLA–PEG multiblock copolymer

PLA–PEG block polymers were synthesized by following the procedures as described in Section 2.2 using (BDI)ZnN(TMS)2 as the catalyst and PEG as initiator. To prepare PLA–PEG diblock copolymer and PLA–PEG–PLA triblock copolymer (LE5 and LE5L, respectively, Table 1), we used mPEG$_{5k}$-OH and HO-PEG$_{5k}$-OH as the corresponding initiator in the presence of (BDI)ZnN(TMS)2.

### 2.4.1. General procedure

In a glove box, mPEG$_{5k}$-OH (50 mg, 0.01 mmol) in anhydrous dichloromethane (DCM, 300 μL) was mixed with a DCM solution of (BDI)ZnN(TMS)2 (6.5 mg, 0.01 mmol, 50 μL). The mixture was stirred for 15 min. A DCM solution of LA (144 mg, 1 mmol, 2.88 mL) was added to the vigorously stirred mPEG$_{5k}$-OH/ (BDI)ZnN(TMS)2 solution. The mixture was stirred at room temperature for 16 h. The conversion of LA was determined by FT-IR by monitoring the lactone band at 1772 cm$^{-1}$. The resulting copolymer LE5 was precipitated with ethyl ether (10 mL), washed with ether and methanol/acetic acid (100/1 (v/v), 10 mL) to remove the BDI ligand, and dried under vacuum. Complete removal of BDI was confirmed by NMR, HPLC and TLC. After the organic solvent was evaporated, the resulting product (LE5) was dissolved in THF (10 mg/mL) and analyzed by GPC. LE5L was prepared and characterized similarly as LE5. The MWs and molecular weight distributions (MWDs) of both LE5 and LE5L were listed in Table 1.

## 2.5. Formation and characterization of Ptxl–LA100/LE5 via sequential precipitation

A DMF solution of Ptxl–LA100 conjugate (50 μL, 2 mg/mL) was added dropwise into a nanopure water solution (2 mL) to give the Ptxl–LA100 NCs. LE5 ($M_n = 1.9 \times 10^4$ g/mol, 2 mg/mL, 100 μL) or mPEG$_{5k}$ (E5, 2 mg/mL, 100 μL) in DMF was added dropwise to the Ptxl–LA100 NCs. A concentrated PBS solution (10×, 228 μL) was added to the nanoprecipitation solution to make the final salt concentration

equivalent to 1× PBS. The NC sizes were measured by DLS. To determine the stability of the NCs in PBS solution, the particle sizes were followed for 30 min by DLS.

## 2.6. Formation and characterization of Ptxl–LA100/LE5 NC via co-precipitation (CPP)

A DMF solution of Ptxl–LA100 conjugate (12 mg/mL, 50 μL) was mixed with a DMF solution of LE5 (12 mg/mL, 50 μL). The mixture was then added dropwise to a vigorously stirred water solution (4 mL). The resulting NCs were analyzed by DLS.

## 2.7. Formation and characterization of Ptxl–LA100/LE5L via co-precipitation

A DMF solution of Ptxl–LA100 (8 mg/mL, 50 μL) was mixed with LE5L in acetone (8 mg/mL, 50 μL). The mixture was then added dropwise to a vigorously stirred water or PBS solution (4 mL). The resulting NCs were analyzed by DLS. The stability of the NCs in the PBS solution was followed for 10–30 min by DLS.

## 2.8. Lyophilization of PLGA–mPEG NPs in the presence of lyoprotectants

An acetone solution of PLGA–mPEG (5 mg/mL, 100 μL) was added dropwise into a vigorously stirred water solution (4 mL) to make the PLGA–mPEG NP. A lyoprotectant was added to the vigorously stirred NC solution at the selected lyoprotectant/ NC mass ratio (varying from 2 to 20). The solution was then lyophilized, reconstituted with 2 mL water and stirred for 5 min. The sizes of the resulting NCs were analyzed by DLS.

## 2.9. Lyophilization of Ptxl–LA100/LE5L NCs in the presence of albumin

An acetone solution of Ptxl–LA100 (4 mg/mL, 50 μL) was mixed with an acetone solution of LE5L (4 mg/mL, 50 μL). The mixture was added dropwise to a vigorously stirred water solution (4 mL). The resulting NC solution was stirred for 6 h in a fume hood to evaporate the acetone; the resulting NC solution was then analyzed by DLS. An aqueous solution of bovine serum albumin (BSA) (12 mg/mL, 500 μL) was added to the NC solution. The mixture was lyophilized for 16 h at −50 °C. The resulting white powder was reconstituted with nanopure water (2 mL) and followed by addition of a concentrated PBS solution (10×, 222 μL). The solution was stirred for 5 min at room temperature. The resulting NC solution was analyzed by DLS.

## 2.10. Conjugation of aptamer to Cy5-LA50/PLA-PEG-COOH NCs

Cy5-LA50 was prepared by following the previously reported procedure [10]. Cy5-LA50/PLA-PEG-COOH NCs (w/w = 1/1, 1 mL, 1 mg/mL in DNase RNase-free water) were incubated with an aqueous solution of 1-(3-dimethylaminopropyl)-3-ethylcarbodimide hydrochloride (EDC) (400 mM, 200 μL) and N-hydroxysuccinimide (NHS) (100 mM, 200 μL) for 15 min at room temperature. The resulting NHS-activated NCs were reacted with 5′-NH2-modified A10 PSMA aptamer (1 μg/μL in DNase RNase-free water, 50 μL). The resulting NC-aptamer bioconjugates were washed with ultrapure water (15 mL) by ultrafiltration (5 min, 1000× g, Ultracel membrane with 10,000 NMWL, Millipore, Billerica, MA, USA). The aptamer-modified NCs were re-suspended (1 mg/mL in DNase RNase-free water) and analyzed by fluorescence-activated cell sorting (FACS, BD FACScan™ Flow Cytometer) and fluorescence microscopy (Leica SP2 Laser Scanning Confocal Microscope).

## 2.11. Analysis of cellular uptake of Cy5-LA50/PLA-PEG-COOH NC-aptamer bioconjugates by fluorescence microscope

LNCaP and PC3 cells were grown in chamber slides in RPMI medium 1640 and F-12 medium (American Type Culture Collection), respectively, supplemented with 100 units/ml aqueous penicillin G, 100 μg/ml streptomycin, and 10% FBS at concentrations to allow 70% confluence in 24 h (i.e., 40,000 cells per cm$^2$). On the day of experiments, the medium was replaced with OptiMEM medium (200 μL) containing Cy5-LA50/PLA-PEG-COOH (w/w = 1/1, 50 μg) NC or Cy5-LA50/PLA-PEG-COOH NC-aptamer (NC-aptamer, 50 μg, 5 wt% of aptamer). The cells and NCs were co-incubated for 2–6 h, after which the cells were washed with PBS (3 × 200 μL), fixed with 4% formaldehyde, counterstained with Alexa-Flour 488 Phalloidin (Invitrogen, CA, USA), mounted and then analyzed on a Leica SP2 Laser Scanning Confocal Microscope at 40× magnification. The images were collected along the z axis with a 0.8-μm interval and reconstructed using the provided software.

## 2.12. Analysis of cellular uptake of Cy5-LA50/PLA-PEG-COOH NC-aptamer bioconjugates by FACS

LNCaP and PC3 cells were grown in 24-well plates in RPMI medium 1640 and F-12 medium (American Type Culture Collection), respectively, supplemented with 100 units/ml aqueous penicillin G, 100 μg/mL streptomycin, and 10% FBS at concentrations to allow 70% confluence in 24 h (i.e., 40,000 cells per cm$^2$). On the day of experiments, cells were washed with prewarmed PBS and incubated with prewarmed phenol-red reduced OptiMEM media for 30 min before the addition of the Cy5-LA50/PLA-PEG-COOH (50 μg) NC or Cy5-LA50/PLA-PEG-COOH NC-aptamer (50 μg, 5 wt% of aptamer). The cells were incubated for 4 h at 37 °C, washed with PBS

**Table 1**
PEG and PEG–PLA copolymers.[a]

| Abbreviation | Name | $M_n$ (×10$^3$ g/mol) | MWD |
|---|---|---|---|
| E5 | mPEG$_{5K}$-OH | 5.3 | 1.01 |
| LE5 | PLA–mPEG$_{5K}$ | 19.3 | 1.09 |
| LE5L | PLA–PEG$_{5K}$–PLA | 34.4 | 1.12 |
| | PLGA–mPEG$_{5K}$ | 18.3 | 1.41 |

[a] $M_n$ = number–average molecular weight; PDI = polydispersity index. Abbreviations of chemicals: mPEG$_{5k}$-OH = mono-methoxy poly (ethylene glycol) with a molecular weight of 5 kDa; PLA = polylactide; PLGA = poly(lactide-co-glycolide) (LA/GA = 50/50 molar ratio).

(2 × 500 µL per well) and subsequently treated with 0.25% trypsin with EDTA for 10 min. The cells were transferred to a 15-mL falcon centrifuge tube and centrifuged at 1200 rpm for 5 min followed by removal of the trypsin solution using a pipette. After the cells were washed with PBS (2 × 500 µL/well), they were fixed with 4% formaldehyde for 10 min at room temperature, washed with PBS (1 × 500 µL) and analyzed by FACS.

## 3. Results and discussion

### 3.1. Synthesis of Ptxl–LA$_{100}$ nanoconjugates

To ensure a rapid and complete polymerization of LA at room temperature using Ptxl as the initiator, we utilized (BDI)ZnN(TMS)$_2$, an active catalyst developed by Coates and coworkers for the polymerization of LA (Fig. 1a) [17]. We have previously reported regioselective initiation of Ptxl followed by controlled polymerization of LA when the polymerization was mediated by (BDI)ZnN(TMS)$_2$ [9]. After Ptxl was mixed with 1 equiv. (BDI)ZnN(TMS)$_2$, the (BDI)Zn-Ptxl alkoxide formed in situ via the 2′-OH of Ptxl (Fig. 1a) initiated and completed the polymerization of LA within hours at room temperature, with nearly quantitative incorporation of Ptxl to the resulting PLA (trace ii, Fig. 2).

Ptxl–LA$_{100}$ was prepared via Ptxl/(BDI)ZnN(TMS)$_2$-mediated LA polymerization at a LA/Ptxl ratio of 100. The obtained $M_n$ of Ptxl–LA$_{100}$ was $1.27 \times 10^4$ g/mol, which is in good agreement with the expected $M_n$ ($1.52 \times 10^4$ g/mol). The Ptxl–LA$_{100}$ also had a very narrow molecular weight distribution (MWD, $M_w/M_n = 1.03$) (Fig. 3), which is consistent with what we reported previously for (BDI)ZnN(TMS)$_2$-mediated regioselective initiation of controlled LA polymerization with Ptxl [9]. Ptxl–LA$_{50}$ and Ptxl–LA$_{200}$, the Ptxl–PLA conjugates prepared at a LA/Ptxl ratio of 50 and 200, respectively, were also synthesized using the same method with expected $M_n$'s and very narrow MWDs. The GPC traces of all three polymers showed monomodal molecular weight distribution patterns (Fig. 3). Syntheses of Ptxl–PLA conjugates are straightforward; gram-scale Ptxl–PLA conjugates with well-controlled composition (Ptxl linked to a PLA chain specifically through its 2′-OH group) and well-controlled MWs can be easily prepared using this drug-initiated polymerization method and utilized for the preparation of NCs. In this paper we report the use of Ptxl–LA$_{100}$ as a model conjugate for development of controlled formulations that are central to clinical translation of nanoparticulate drug delivery systems.
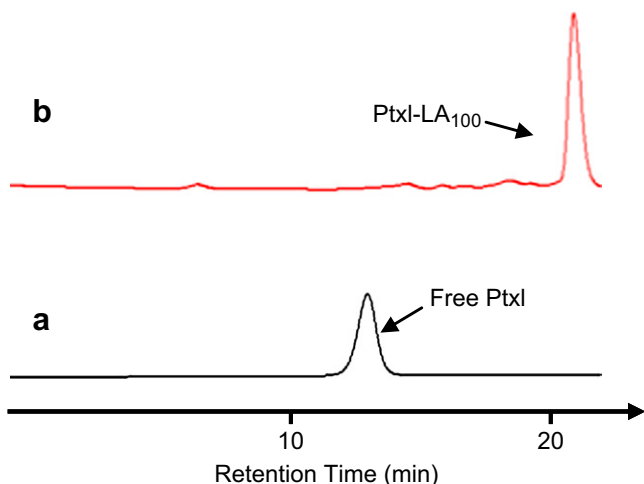


**Fig. 2.** HPLC spectrum of (a) free Ptxl and (b) the solution of Ptxl/(BDI)ZnN(TMS)$_2$-mediated LA polymerization at a LA/Ptxl ratio of 100. An aliquot (30–50 µL) of polymerization solution was injected into HPLC equipped with analytical RP-HPLC column (Curosil-PFP, 4.6 × 250 mm, 5 µ, Phenomenex, Torrance, CA). Mobile phase was acetonitrile/water with 0.1% TFA (50/50 (v/v)); the flow rate was set at 1.0 mL/min.
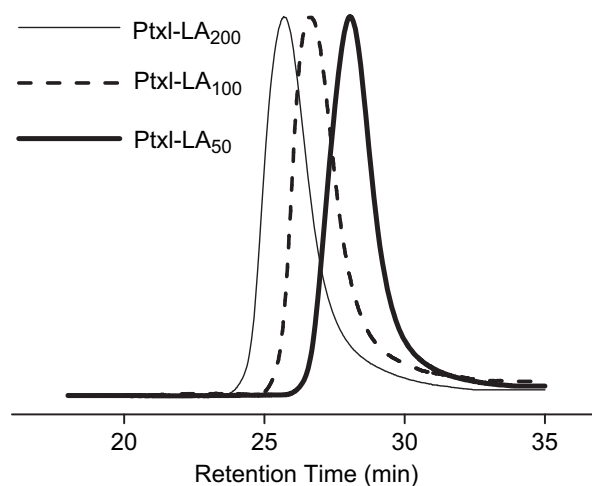


| [LA]/[Ptxl] | $M_{cal}$ (×10$^3$g/mol) | $M_n$ (×10$^3$g/mol) | MWD |
|---|---|---|---|
| 50 | 8.1 | 7.8 | 1.04 |
| 100 | 15.3 | 12.7 | 1.03 |
| 200 | 29.7 | 28.1 | 1.02 |

**Fig. 3.** GPC analysis of Ptxl–LA$_{200}$, Ptxl–LA$_{100}$ and Ptxl–LA$_{50}$.

### 3.2. Formation of Ptxl–LA$_{100}$ nanoconjugates via nanoprecipitation (NPP)

Nanoprecipitation (NPP) is an extensively used method for the preparation of NPs with therapeutic agents embedded in the hydrophobic polymeric matrices [13,22]. This method allows for rapid access to NPs in large quantity. Typically, a mixture of hydrophobic polymer and drug is dissolved in water-miscible organic solvent (e.g., DMF or acetone) and then added dropwise to a vigorously stirred water solution ($V_{water}/V_{solvent} = 10–40$). The instantaneous diffusion of the organic solvent into water results in formation of polymer/drug NPs.

The NPP of Ptxl–LA$_{100}$ resulted in sub-100 nm Ptxl–LA$_{100}$ NCs with monomodal particle size distributions and low polydispersities (Fig. 4). In hundreds of NPP experiments that we have performed using Ptxl–PLA conjugates with various MWs, we rarely observed NCs with more than one particle size distribution based on the DLS analysis. The narrow, monomodal particle size distributions for NCs derived from NPP of the Ptxl–PLA conjugates have also been confirmed by SEM analysis in our previous study [9], and are in sharp contrast to the multimodal particle size distribution typically observed with the NPs prepared by the co-precipitation (CPP) of a mixture of Ptxl and hydrophobic polymer (e.g., PLA or PLGA (poly(lactide-co-glycolide))) [13]. As the multimodal distribution of NPs is due in part to the aggregation of the non-encapsulated drug molecules [13], the monomodal particle size distribution pattern observed and very low polydispersities with the Ptxl-LA$_{100}$ NCs are likely related to the unimolecular structures of the Ptxl–PLA conjugates.

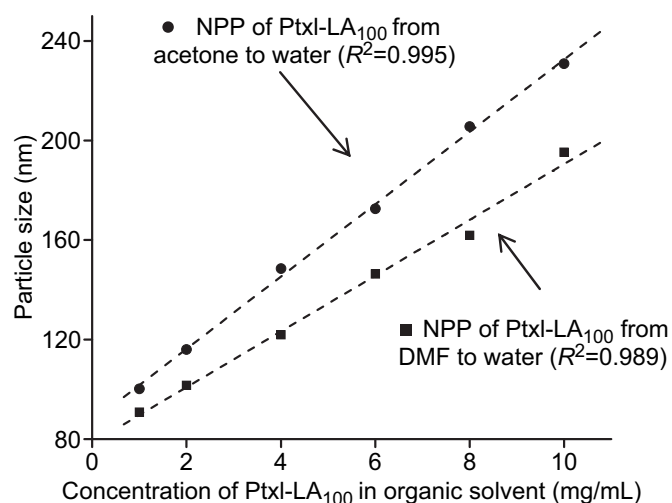### 3.3. Control of Ptxl–LA$_{100}$ NC size in the NPP process (Approach i, Fig. 1b)

Particle size is one of the most important parameters of NPs and has significant impact on biodistribution, clearance kinetics, and in vivo efficacy [6,23]. With respect to biodistribution, the upper limit of desirable NP size is typically around 200 nm. Particles with diameters of 200 nm or greater are more likely to induce an
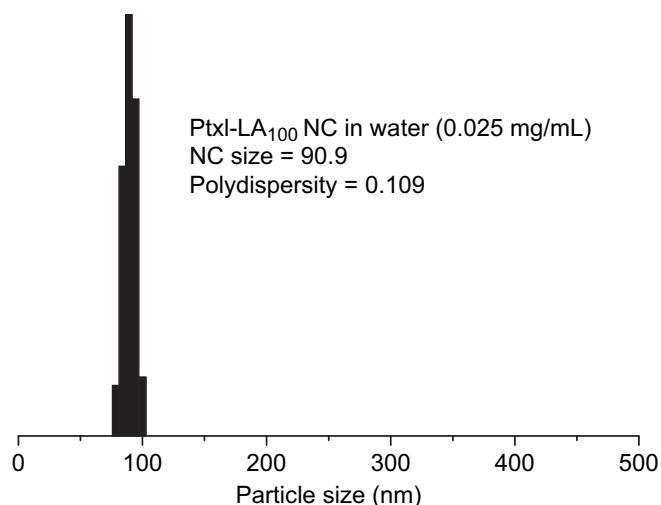
Fig. 4. Dynamic light scattering (DLS) analysis of Ptxl–LA$_{100}$ NC in water (0.025 mg/mL).



Fig. 5. Ptxl–LA$_{100}$ NC size versus the concentration of Ptxl–LA$_{100}$ with the use of acetone (●) or DMF (■) as the solvent for nanoprecipitation. The volume ratio of organic solvent to water was fixed at 1/40. The dashed line indicates the linear correlation of the NC size with the concentration of Ptxl–LA$_{100}$. $R^2$ is the linear correlation constant of the corresponding system.

immune response and be taken up by the Kupffer cells than their smaller counterparts, resulting in rapid clearance of particles from circulation [3]. Particles 150 nm or smaller can escape through fenestration of the vascular endothelium and be cleared from circulation, while particles smaller than 10 and 30 nm are easily cleared through the kidney or lymph nodes, respectively [3]. Although it is still not entirely clear which NP size leads toward the most favorable biodistribution and highest therapeutic efficacy *in vivo* when NPs are systemically administered, there is a general consensus that NPs should be controlled below 200 nm [3]. Previous studies have revealed that NPs with diameters less than 200 nm can passively accumulate in solid tumor through the enhanced permeation retention effect (EPR) [24], a mechanism that has been broadly utilized to improve the residence of NPs in tumor tissues. However, NPs with sizes below 200 nm may still behave dramatically different in different size ranges in terms of their *in vivo* biodistribution, tumor targeting efficiency, tumor penetration and anticancer efficiency [7]. One goal of this research project is to develop NCs with various size ranges as a tool to facilitate the evaluation of the correlation of the biodistribution and anticancer efficacy of NCs with NC size. Such information can be subsequently utilized for *in vivo* targeted cancer therapy. To achieve this goal, it is essential to develop methods that allow for facile formulation of NCs with precisely-controlled sizes. For this reason, we performed a series of studies using Ptxl–LA$_{100}$ as a model PLA-drug conjugate to assess how solvent, concentration of Ptxl–LA$_{100}$ and surfactant would affect the sizes of NCs and how NCs could be prepared with no or negligible aggregation in PBS solution for an extended period of time to facilitate their *in vivo* applications.

We first studied the effect of solvent on the NPP of Ptxl–LA$_{100}$ with water as the non-solvent. Previous studies by us [13] and others [25,26] showed that the miscibility of the organic solvent with water can dramatically impact NP size in a given solvent/water system. As shown in Fig. 5, the sizes of Ptxl–LA$_{100}$ NCs and the water-miscibility of the two organic solvents used in this study were well correlated; an increase of water-miscibility led to a decrease in the mean NC size when all other formulation parameters were held constant. Ptxl–LA$_{100}$ NCs prepared with DMF as the solvent, a more water-miscible solvent, resulted in smaller particles. This is presumably due to more efficient solvent diffusion and polymer dispersion into water in this DMF/water NPP system. The Ptxl–LA$_{100}$ NCs prepared with acetone, a less water-miscible solvent than DMF, were typically 20–30 nm larger than the NCs

prepared with DMF as the solvent at the corresponding concentration (Fig. 5). Acetone can be readily removed by evaporation because of its low boiling point. In contrast, DMF has to be removed by ultrafiltration followed by extensive washing. Thus, NC formulation via NPP in the acetone/water system is much easier, which is more suitable for the large-scale preparation of NCs.

We next studied the effect of the Ptxl–LA$_{100}$ concentration during NPP on the size of NCs. When the polymer concentrations were varied during the NPP of Ptxl–LA$_{100}$ at a fixed solvent:water ratio (Fig. 5), we observed a linear correlation of NC size with the Ptxl–LA$_{100}$ concentration. The sizes of the NC increased from 90.9 nm to 195.3 nm as the polymer concentration in DMF increased from 1 mg/mL to 10 mg/mL. Similar correlation was also observed with acetone as the solvent for the NPP of Ptxl–LA$_{100}$ (Fig. 5). In both DMF/water and acetone/water NPP systems, the polydispersities of the NCs at all concentrations remained very low, ranging 0.061–0.128 and 0.081–0.168 for NCs derived from DMF/water and acetone/water system, respectively. Because of the linear correlation of NC size with the concentration of Ptxl–PLA conjugate during NPP, NCs with any desirable sizes ranging from 80 to 250 nm can be obtained simply by adjusting precipitation concentration.

### 3.4. Formation of NCs via sequential precipitation of Ptxl–LA$_{100}$ and LE5 (Approach ii, Fig. 1b)

NCs are designed specifically for *in vivo* drug delivery applications. It is desirable to have NCs with prolonged circulation to maximize their therapeutic efficacy. To achieve protracted retention in circulation with reduced recognition by reticuloendothelial system, both the size and surface properties of NCs have to be well-controlled [3]. Systemically administered NPs without proper surface modification are usually cleared rapidly from the circulation and localized predominantly in liver and spleen [13,27]. Severe liver and spleen retention greatly diminishes the accessibility of the NPs to tumor tissues and also causes liver and spleen damage. The clearance is due to the scavenging by liver Kupffer cells and spleen macrophages [3]. NP surface properties play a critical role in the blood opsonization, a process involving the deposition of protein opsonins that are recognized by phagocytic cells, thereby accelerating the clearance of NPs from blood. Opsonization of NPs can be

substantially reduced when NP surface features are properly controlled [28]. Modification of NP surfaces with PEG, termed "PEGylation", is a well-established approach to reduce protein binding [29]. Suppression of opsonization is thus achievable by PEGylation and has been utilized to enhance the circulation half-life of NPs from several minutes to several or tens of hours [16,23,30]. Since the report of long-circulating NP [23], surface PEGylation has been extensively used to prepare *in vivo* applicable drug delivery systems [29] and other biotechnology applications [31,32].

Ptxl–LA$_n$ NCs have negative surface zeta-potential and remain non-aggregated in water due to surface charge repulsion. However, aggregation of NCs occurred in PBS, presumably due to salt-induced screening of the repulsive force (Fig. 6a) [33,34]. The popular PEGylation strategy was thus adopted in this study to create NCs that will not aggregate in salt solution. PEGylated NCs likely also have reduced protein binding for their *in vivo* applications.

PEG is typically covalently conjugated to the surface of NPs [13,22]. To minimize efforts involved in conjugation chemistry, we attempted a direct deposition method to coat NC with PEG. PLA–mPEG$_{5k}$ (LE5, Table 1), an amphiphilic block copolymer with PLA block of 14 kDa and mPEG segment of 5 kDa, was synthesized via

the ring-opening polymerization of LA using a mixture of mPEG and (BDI)ZnN(TMS)$_2$. Dropwise addition of LE5 to the Ptxl–LA$_{100}$ NC aqueous solution resulted in rapid coating of Ptxl–LA$_{100}$, presumably via the hydrophobic interaction of PLA segment of LE5 and the hydrophobic NC surface. After treatment, the size of the Ptxl–LA$_{100}$ NC increased from 101.6 nm to 112.7 nm. The resulting NCs remained non-aggregated for at least 30 min in PBS (Fig. 6a). To demonstrate the importance of the PLA block to the non-covalent surface PEGylation, we added mPEG5k (E5, Table 1) to the NC solution followed by the addition of PBS. Without the hydrophobic PLA block, E5 should not form stable interaction with NCs. As expected, Ptxl–LA$_{100}$/E5 NCs formed large aggregates almost instantaneously after PBS was added, following a very similar aggregation pattern as the parental NCs in PBS (Fig. 6a). Furthermore, analyses of the Ptxl–LA$_{100}$ NC by DLS before and after treatment showed that particles retained their monomodal distribution pattern (Fig. 6b). The DLS experiments indicated that LE5 favorably precipitated on the surface of Ptxl–LA$_{100}$ NCs instead of self-assembling to form micelles. The resulting PEG coated NCs form a core-shell nano-structure with hydrophobic polymer-drug conjugate being in the core and LE5 on the shell, which has been confirmed by various TEM studies (to be reported).

### 3.5. Formation of NCs via co-precipitation of mixtures of Ptxl–LA$_{100}$ and LE5 (Approach iii, Fig. 1b)

Formation of Ptxl–LA$_{100}$/LE5 core-shell type nanostructures requires two steps to finish – the NPP of Ptxl–LA$_{100}$ to form NC core followed by coating with LE5 to form the PEG shell. Preparation of salt-stable NCs in such a step-wise manner is difficult to handle, especially for the preparation of NCs in large scale. It is desirable to formulate salt-stable Ptxl–LA$_n$ NCs in one step. We next tested whether we could formulate salt-stable NCs by co-precipitating (CPP) a mixture of Ptxl–LA$_{100}$ and LE5.

We mixed Ptxl–LA$_{100}$ with LE5 at 1:1 mass ratio in DMF, a fixed ratio utilized throughout the studies reported in this paper, and then precipitated them in nanopure water ($V_{DMF}/V_{water} = 1/40$). Linear increase in particle size with the increase of polymer concentration was observed (Fig. 7a), following a similar trend as the NPP of Ptxl–LA$_{100}$ previously discussed in Fig. 5. The sizes of NCs gradually increased from 61.4 nm to 121.0 nm when the concentration of Ptxl–LA$_{100}$ increased from 2 mg/mL to 10 mg/mL. When acetone was used as the solvent, similar linear correlation of NC sizes with the concentration of Ptxl–LA$_{100}$ was observed. The sizes of NCs increased from 79.2 to 145.9 nm when the concentration of Ptxl–LA$_{100}$ increased from 2 mg/mL to 10 mg/mL. The NCs obtained in the latter case (CPP of Ptxl–LA$_{100}$/LE5 from acetone to water) were roughly 20–25 nm larger than the NCs prepared with DMF as solvent at corresponding concentration, similar to the solvent effect described in Fig. 5. NCs prepared in both DMF/water and acetone/water systems showed narrow-dispersed, monomodal particle size distribution, exemplified by the Ptxl–LA$_{100}$/LE5 NC prepared via the NPP with a concentration of 6 mg/mL in acetone (Fig. 7b). We next evaluated the stability of the NCs in PBS. After precipitating a mixed DMF solution of Ptxl–LA$_{100}$ and LE5 (Ptxl–LA$_{100}$ = 4 mg/mL) in a water solution ($V_{DMF}/V_{water} = 1/40$) followed by the addition of PBS to the resulting NC solution, the particles remained non-aggregated for an extended period of time based on the DLS analyses (data not shown).

### 3.6. Formation of NCs via co-precipitation of mixtures of Ptxl–LA$_{100}$ and LE5L (Approach iv, Fig. 1b)

To further simplify NC formulation, we explored whether it was possible to formulate stable NCs directly in PBS solution.
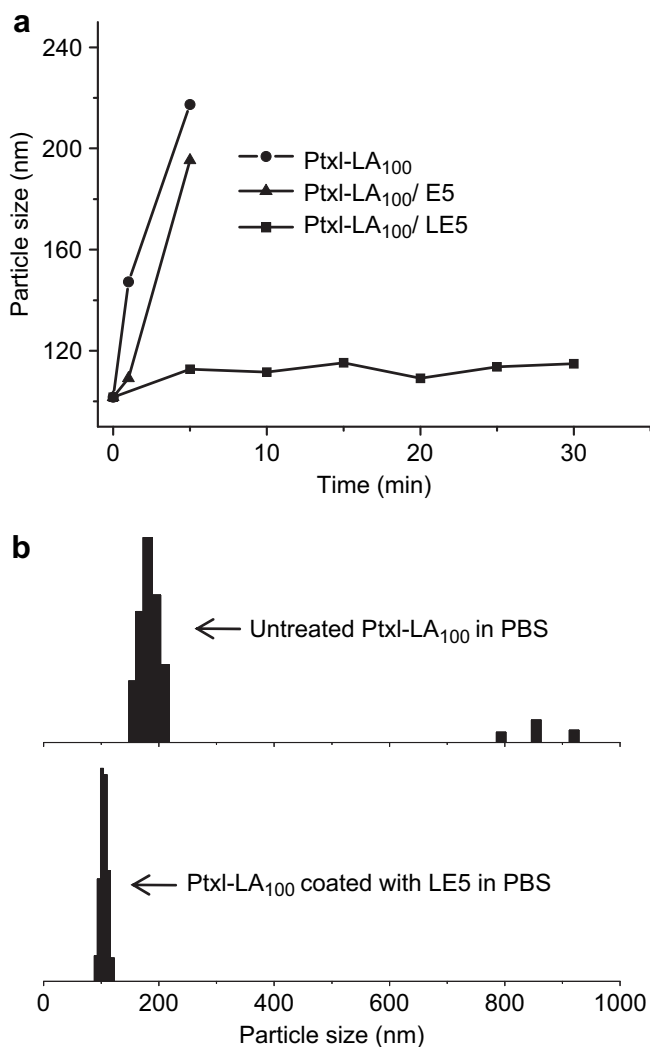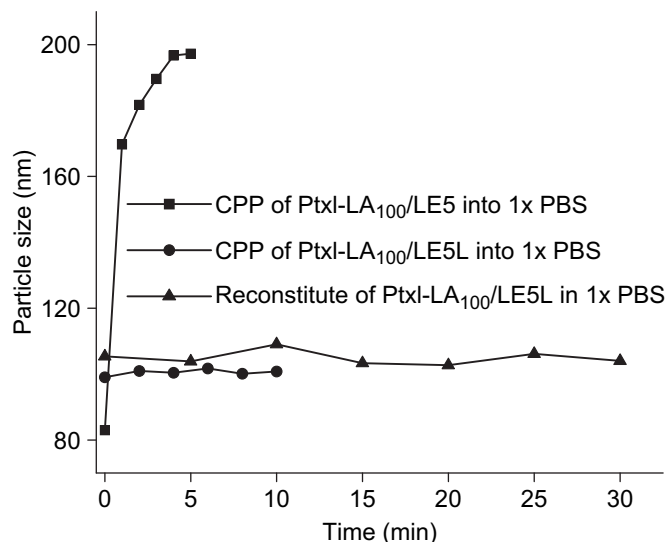


**Fig. 6.** (a) Stability of Ptxl–LA$_{100}$ NCs in PBS (1×) after coating with mPEG$_{5k}$ (E5) or with PLA–mPEG$_{5k}$ (LE5). (b) DLS spectra of Ptxl–LA$_{100}$/LE5 NCs and untreated Ptxl–LA$_{100}$ NCs. Particle sizes were determined 4 min after particles were present in PBS solution.
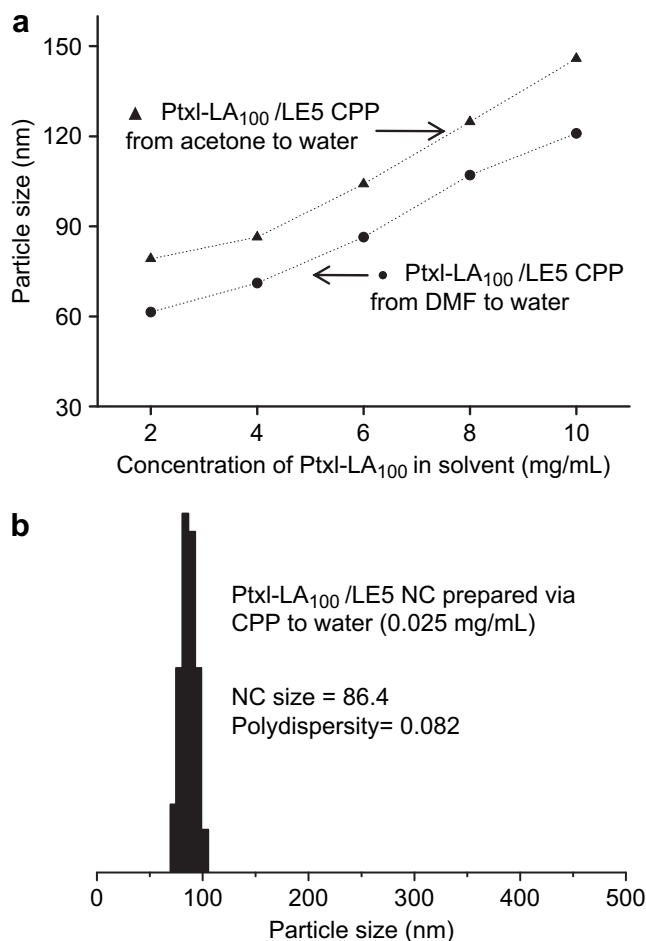
**Fig. 7.** (a) Co-precipitation (CPP) of Ptxl–LA$_{100}$/LE5 (wt/wt = 1/1) from DMF or acetone solution into water at various Ptxl–LA$_{100}$ concentrations. (DMF (or acetone)/water = 1/40 (v/v)). (b) Ptxl–LA$_{100}$/LE5 NC size distribution determined by DLS. Condition: Ptxl–LA$_{100}$ in DMF (50 μL, 12 mg/mL) was mixed with a DMF solution of LE5 (50 μL, 12 mg/mL). The mixture was added dropwise to a vigorously stirred water solution (4 mL). The resulting Ptxl–LA$_{100}$/LE5 NCs was analyzed by DLS.



**Fig. 8.** The stability of NCs in PBS solution. ■: A mixture of Ptxl–LA$_{100}$ and LE5 in DMF (w/w = 1/1, Ptxl–LA$_{100}$ = 4 mg/mL) was co-precipitated in 1× PBS (DMF/PBS = 1/40 (v/v)). ●: A mixture of Ptxl–LA$_{100}$ and LE5L in DMF (w/w = 1/1, Ptxl–LA$_{100}$ = 4 mg/mL) was co-precipitated in 1× PBS (DMF/PBS = 1/40 (v/v)). ▲: A mixture of Ptxl–LA$_{100}$ and LE5L in acetone (w/w = 1/1, Ptxl–LA$_{100}$ = 2 mg/mL, 100 μL) was co-precipitated in water (4 mL). The obtained NC had a diameter of 88.9 nm with a polydispersity of 0.092. The resulting NC solution was mixed with an aqueous solution of BSA (500 μL, 12 mg/mL) and the mixture was lyophilized for 16 h at −50 °C. The resulting powder was reconstituted with 2-mL water followed by the addition of a concentrated PBS solution (222 μL, 10×). The mixture was stirred for 5 min at room temperature and analyzed by DLS.

When the mixture of Ptxl-LA$_{100}$ and LE5 was directly co-precipitated in PBS, the resulting NCs were not stable in PBS and formed large aggregates rapidly (Fig. 8). The particle size increased from 83 nm to 197 nm within 6 min. Interestingly, when LE5L (Table 1), an ABA type triblock copolymer with PEG as the B clock (MW = 5 kDa) and PLA as the A block (MW = 14 kDa), was mixed with Ptxl-LA$_{100}$ at 1:1 mass ratio in DMF and subsequently precipitated in PBS, the resulting Ptxl–LA$_{100}$/LE5L NCs were found to be surprisingly stable in PBS and remained non-aggregated for an extended period of time (Fig. 8). To compare the non-solvent effect on the NC formulation, we conducted CPP of Ptxl–LA$_{100}$/LE5L at various concentrations in both PBS and water. When water was used as the non-solvent, the size of the Ptxl–LA$_{100}$/LE5L NC gradually increased from 66.8 nm to 125.5 nm as the concentration of the mixture increased from 2 mg/mL to 10 mg/mL. CPP of the Ptxl–LA$_{100}$ and LE5L mixture in water or to PBS showed a linear correlation of Ptxl–LA$_{100}$ concentration with NC size (Fig. 9), similar to the NPP of the Ptxl–LA$_{100}$ in water reported previously (Fig. 5). When the CPP was performed with PBS as the non-solvent, the sizes of NCs were typically 20–40 nm larger than those derived from the NPs prepared with water as the non-solvent and followed a linear trend with the concentration of Ptxl–LA$_{100}$; the sizes of NCs increased from 99.0 to 156.5 nm when

the concentration of the of Ptxl–LA$_{100}$ in the mixture increased from 2 mg/mL to 10 mg/mL (Fig. 9). NCs prepared at various concentrations all stayed non-aggregated in PBS for an extended period of time (data not shown). It is known that triblock LE5L and diblock LE5 self-assemble in different manners. LE5 forms star-like micelles, while LE5L, because of its ABA type of amphiphilic structure, tends to form flower-like micelles (Fig. 1b) [35]. Hydrophobic polymer chains in flower-like micelles tend to have stronger interaction than those in star-like micelles, which may in part contribute to the formation of Ptxl–LA$_{100}$/LE5L NCs with stably coated PEG shell and enhanced stability in the PBS solution. The detailed mechanism of Ptxl–LA$_{100}$/LE5L and Ptxl–LA$_{100}$/LE5 NC self-assembly is yet to be determined.
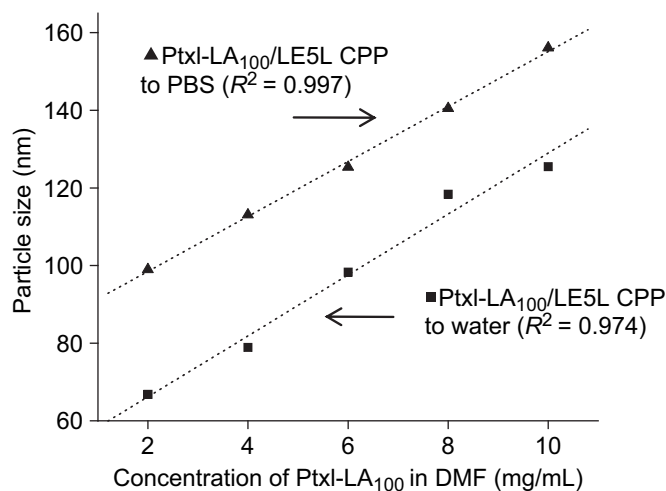


**Fig. 9.** Linear correlation of Ptxl–LA$_{100}$/LE5L NC size with Ptxl–LA$_{100}$ concentration in DMF when the mixture of Ptxl–LA$_{100}$/LE5L was co-precipitated in water or in PBS.

### 3.7. Lyophilization and storage of Ptxl–PLA NCs

Formulations of small-scale NPs that stay non-aggregated in PBS for *in vitro* or *in vivo* laboratory studies are relative easy to control. However, in order to facilitate their clinical translation, NPs have to be prepared in large quantity with well-controlled properties, which should remain unchanged during the processes of manufacturing, storage and transport prior to their use in clinic. In Ptxl–PLA, because Ptxl is covalently conjugated to PLA through an ester bond that is subject to hydrolysis upon exposure to water, handling of NCs in aqueous solution in the abovementioned processes is undesirable. NCs have to be formulated in solid form in order for them to be used in clinic.

It is known that PLA-based NPs tend to aggregate during lyophilization. As expected, when the Ptxl–$LA_{100}$/LE5 or the Ptxl–$LA_{100}$/LE5L NCs with sub-100 nm sizes were lyophilized, reconstituted and re-analyzed by DLS, micrometer-sized, non-dispersible aggregates were observed. Administration of polymeric NPs with micron size aggregates via tail vein injection led to instantaneous mice death based on our previous experience (unpublished data).

There have been many studies using lyoprotectants to physically separate NP from aggregating during lyophilization. Mono- or di-saccharides, such as sucrose, dextrose, maltose, sorbitol, glucose, are frequently used as lyoprotectants because their biocompatibility and low cost [36]. In our previous efforts of developing aptamer-based cancer targeting and therapy, we conducted preliminary studies on the lyophilization of PLGA–$mPEG_{5k}$ NPs with the use of sucrose as the lyoprotectant [13]. Although the aggregation of PLGA–$mPEG_{5k}$ NPs was reduced during lyophilization, formation of substantial amount of large, non-dispersible aggregates was still observed. Based on this previous study, we screened a large number of lyoprotectants using PLGA–$mPEG_{5k}$ based NPs and compared them with sucrose for their capabilities of preventing NP aggregation during lyophilization (Table 2).

PLGA–$mPEG_{5k}$ NPs were prepared via nanoprecipitation of PLGA–$mPEG_{5k}$ (Table 1) as previously described in ref. [13]. Commonly used saccharide-based lyoprotectants, such as sucrose, sorbitol, maltose, dextrose and mannose, were able to reduce NP aggregation to some degree when the NPs were lyophilized along with these lyoprotectants (Table 2). High lyoprotectant chemical/NP mass ratio ($W_C/W_{NP}$, Table 2) was more effective in terms of reducing NP aggregation (Table 2). However, even at a $W_C/W_{NP}$ ratio as high as 10, significant NP aggregations were observed in all systems (Table 2). DLS analyses of these NPs after lyophilization showed multimodal particle size distributions. Some large, non-dispersible aggregates precipitated from the solution and were even visible with the naked eye. Other sugars, such as galactose, could not prevent NP aggregation at all even at a lyoprotectant/NC mass ratio of 10. We also tested whether amino acid (e.g., glycine) or surfactant (e.g., SDS) could be used as the lyoprotectant and found that they were unable to prevent NP aggregation during lyophilization (Table 2).

Because none of the small molecules tested could effectively prevent NP aggregation during lyophilization, we next tested whether macromolecules could provide better lyoprotection during NP lyophilization. Albumin, an abundant protein in blood, has attracted much interest in drug delivery recently. Abraxane®, an albumin–paclitaxel NP, has been recently approved by the US Food and Drug Administration for cancer treatment [37]. We tested whether bovine serum albumin (BSA) could be used as a lyoprotectant of NPs. At a BSA/NP mass ratio of 2, the NP size increased by 8.2 times from 62 nm before lyophilization to 512 nm after lyophilization; two particle size distributions were observed. When the BSA/NP mass ratio increased to 6 and 10, the size of the lyophilized NP became 176 nm and 114 nm, respectively. This

**Table 2**
Characterization of PLGA–mPEG NPs lyophilized in the presence of various lyoprotectant and reconstituted by water[a].

| Lyoprotectant[b] | $W_C/W_{NP}$[c] | Size in nm (STD)[d] | PDI (STD)[d] | Distrib. Num.[e] | $S_L/S_O$[f] | Aggr.[g] |
|---|---|---|---|---|---|---|
| Sucrose | 2 | 245.2 (2.1) | 0.227 (0.003) | 2 | 3.93 | Y |
| Sucrose | 10 | 217.5 (3.0) | 0.220 (0.002) | 2 | 3.49 | Y |
| Sorbitol | 2 | >1000 | >1000 | N.D. | N.D. | Y |
| Sorbitol | 10 | 764.8 (39.2) | 0.299 (0.021) | 2 | 12.28 | Y |
| Maltose | 2 | >1000 | >1000 | N.D. | N.D. | Y |
| Maltose | 10 | 220.4 (3.2) | 0.288 (0.008) | 2 | 3.54 | Y |
| Dextrose | 2 | 250.4 (9.5) | 0.345 (0.0120 | 2 | 4.02 | Y |
| Dextrose | 10 | 79.1 (2.3) | 0.075 (0.032) | 2 | 1.26 | Y |
| Mannose | 2 | >1000 | >1000 | N.D. | N.D. | Y |
| Mannose | 10 | 245.2 (1.6) | 0.254 (0.011) | 2 | 3.93 | Y |
| Galactose | 10 | >1000 | >1000 | N.D. | N.D. | Y |
| Glycine | 10 | >1000 | >1000 | N.D. | N.D. | Y |
| SDS | 10 | >1000 | >1000 | N.D. | N.D. | Y |
| BSA | 2 | 511.8 (24.7) | 0.392 (0.005) | 2 | 8.21 | Y |
| BSA | 6 | 175.9 (3.3) | 0.343 (0.008) | 1 | 2.82 | N |
| BSA | 10 | 114.1 (1.4) | 0.110 (0.002) | 1 | 1.83 | N |

[a] In this study PLGA–$mPEG_{5k}$ ($M_n = 19.4 \times 10^3$ g/mol) was used to study the efficiency of lyoprotectant. The original PLGA–mPEG NP had a diameter of 62.7 nm, which was formulated through the NPP of PLGA–mPEG to water. After the NPP was complete, the corresponding lyoprotectant was added as the selected lyoprotectant/NP mass ratio prior to lyophilization.
[b] SDS = sodium dodecyl sulfate; BSA = bovine serum albumin.
[c] $W_C/W_{NP}$ = the mass ratio of lyoprotectant chemicals versus. NP.
[d] PDI = polydispersity; STD = standard deviation.
[e] Distrib. Num. = the number of particle size distribution. N.D. = not determined.
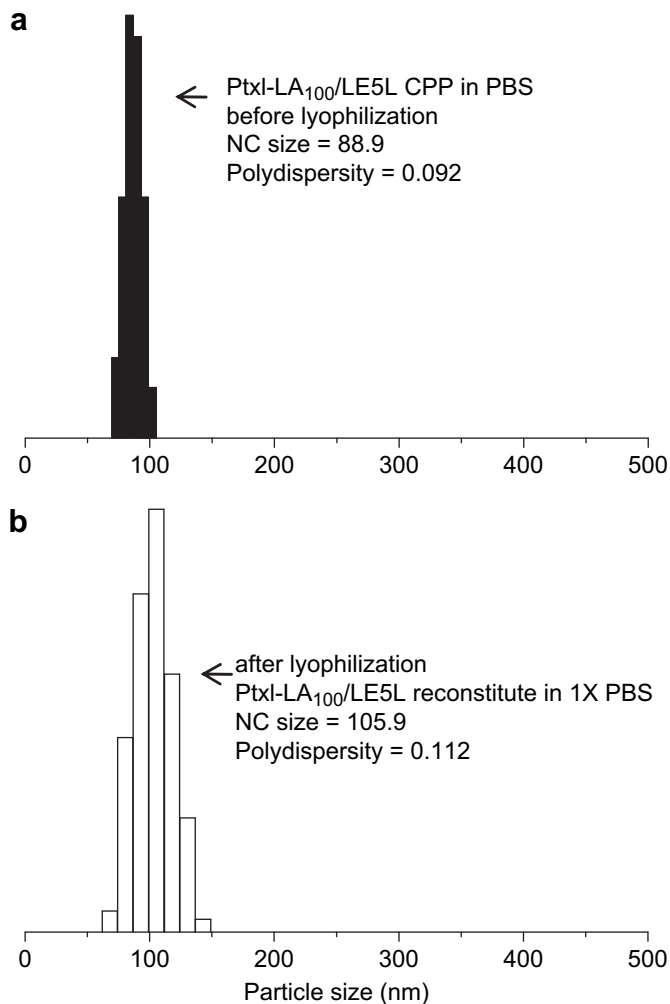[f] $S_L/S_O$ = the ratio of the lyophilized NP size to pre-lyophilized NP size.
[g] Aggr. = visible large aggregates; Y = aggregates observed; N = no aggregates observed.

corresponds to roughly 2.8- and 1.8-times the pre-lyophilized NPs. For the first time we were able to completely disperse the lyophilized NPs with sub-200 nm diameters and absolutely no precipitates. The reconstituted NPs showed monomodal particle size distribution as determined by DLS (data not shown).

We next tested whether albumin could be used to stabilize Ptxl–$LA_{100}$/LE5L NC. A Ptxl–$LA_{100}$/LE5L NC was first prepared by co-precipitation as described previously in Fig. 9. The particles size and the polydispersity of the resulting NC were 88.9 nm and 0.092, respectively, as determined by DLS. After lyophilization at a BSA/NC mass ratio of 15 followed by reconstitution with 1× PBS, the NC size increased slightly to 105.9 nm (Fig. 10) but remained non-aggregated for at least 10 min during the course of DLS analysis. Monomodal particle size distribution was verified by DLS analysis (Fig. 10). The polydispersity of NCs remained as low as 0.112. This experiment has been repeated multiple times with consistent and highly reproducible results and no NC aggregation in each of the repeated experiments. Because of the biocompatibility of albumin, this albumin-based lyoprotection strategy may be broadly used in solid formulations for drug delivery or other translational applications.

### 3.8. Ptxl–PLA NCs for prostate cancer targeting

Aptamers are either single-stranded DNA or RNA that specifically bind to a target ligand or ligands. They were selected from

**a**



Ptxl-LA$_{100}$/LE5L CPP in PBS
before lyophilization
NC size = 88.9
Polydispersity = 0.092

**b**



after lyophilization
Ptxl-LA$_{100}$/LE5L reconstitute in 1X PBS
NC size = 105.9
Polydispersity = 0.112

Particle size (nm)

**Fig. 10.** (a) DLS spectrum of NC obtained from the co-precipitation of an acetone solution of Ptxl–LA$_{100}$/LE5L (w/w = 1/1, Ptxl–LA$_{100}$ = 2 mg/mL, 100 μL) in water (4 mL, acetone/water = 1/40 (v/v)). The obtained NC had a diameter of 88.9 nm with a polydispersity of 0.092. (b) The resulting NC solution was then mixed with an aqueous solution of BSA (500 μL, 12 mg/mL) and the mixture was lyophilized for 16 h at −50 °C. The resulting powder was reconstituted with 2-mL water followed by the addition of a concentrated PBS solution (222 μL, 10×). The mixture was stirred for 5 min at room temperature and analyzed by DLS. The obtained NC had a diameter of 105.9 nm with a polydispersity of 0.112.

a library of nucleic acids with random sequences via a combinatorial process called Systematic Evolution of Ligands by Exponential Enrichment (SELEX) [38–40]. When used for cancer targeting, aptamers are capable of binding to target antigens with extremely high affinity and specificity in a manner resembling antibody-mediated cancer targeting. Aptamers are typically non-immunogenic and exhibit remarkable stability against pH, temperature and solvent. Synthesis of aptamers is an entirely chemical process and thus shows negligible batch-to-batch inconsistency [41]. These unique properties of aptamers are in sharp contrast to antibodies that are typically unstable against temperature and pH change, are immunogenetic, and have significant batch-to-batch variability.

An A10 aptamer with 2′-fluoro-modified ribose on all pyrimidines and a 3′-inverted deoxythymidine cap has been identified via SELEX and utilized to target extracellular prostate-specific membrane antigen (PSMA) [42]. It binds to the PSMA-positive LNCaP prostate cancer cells but not PSMA-negative PC3 prostate cancer cells. Previous study showed that PLGA-A10 aptamer bioconjugates were capable to target LNCaP cells *in vitro* and *in vivo* [22,43].

Cy5 (a fluorescence dye with hydroxyl groups) was used to initiate LA polymerization to prepare Cy5-PLA and subsequently Cy5-PLA NCs for study of the *in vitro* cancer targeting. The amine-terminated A10 aptamer was conjugated to the PLA-PEG-COOH/Cy5-PLA NCs (particle size was 132.8 nm with the polydispersity of 0.031) through the carboxylic acid-amine coupling reaction in the presence of EDC and NHS to give aptamer/PLA-PEG-COOH/Cy5-PLA NCs (aptamer-Cy5 NC) [43]. After purifying the aptamer-Cy5 NCs by centrifugation and washing the NCs with PBS, we found that the size of aptamer-Cy5 NCs increased slightly to 157.1 nm with a polydispersity of 0.144 after conjugation of the A10 aptamer. Freshly prepared aptamer-Cy5 NCs were then applied to the LNCaP (PSMA+) and PC-3 (PSMA−) cells, and their binding and internalization were assessed by FACS (Fig. 11). As shown in Fig. 11a, the mean fluorescence intensity of the LNCaP cells (PSMA+) incubated with aptamer-Cy5 NC for 4 h was 376.7 (arbitrary intensity unit on FACS Cy5 channel), as compared to 72.4 for PS3 cell (PSMA-) and 16.4 in the untreated LNCaP cells. The fluorescence intensity of the aptamer-Cy5 NC treated LNCaP cells was 5.2 times higher than that of PC-3 cells treated under the same condition, indicating enhanced aptamer-Cy5 NC binding to PSMA+ LNCaP cells and potentially improved NC internalization. A kinetic study for the internalization of aptamer-Cy5 NCs into LNCaP cells was then performed (Fig. 11b). The LNCaP cells treated with aptamer-Cy5 NCs for 2 h revealed a mean fluorescence intensity of 136.2, as compared to 16.4 of the untreated cells. When the LNCaP cells were treated with aptamer-Cy5 NCs for 6h, the mean fluorescence intensity increased to 779.8, indicating 5.7 times more NCs were internalized into the cells. Those observations were confirmed by an uptake imaging study using confocal microscopy. As shown in Fig. 12, the uptake of Cy5 NCs to LNCaP cells was significantly enhanced when NCs were coated with aptamer. Incubation of aptamer-Cy5 NCs with LNCaP cells for longer time resulted in substantially increased NC internalization. Because PC-3 cells do not express the PSMA protein, there was essentially no
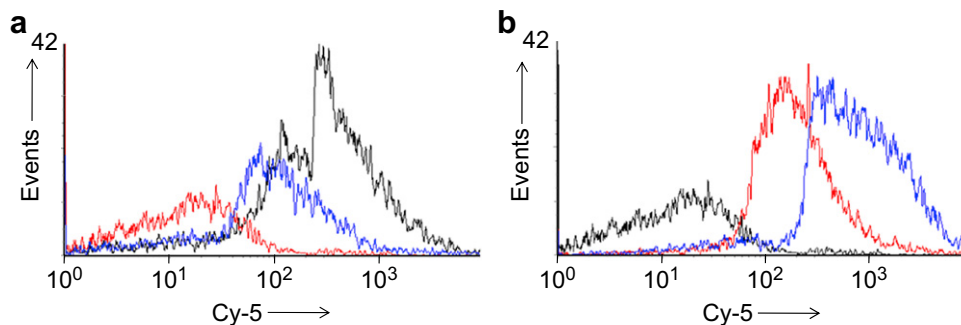


**Fig. 11.** Flow cytometry analysis of NP–Apt conjugates cellular uptake. (a) Untreated LNCaP cells (red line); PC3 cells treated with NP–Apt for 4 h (blue line); LNCaP cells treated with NP–Apt for 4 h. (b) Untreated LNCaP cells (black line); LNCaP cells treated with NP–Apt for 2 h (red line) and 6 h (blue line).
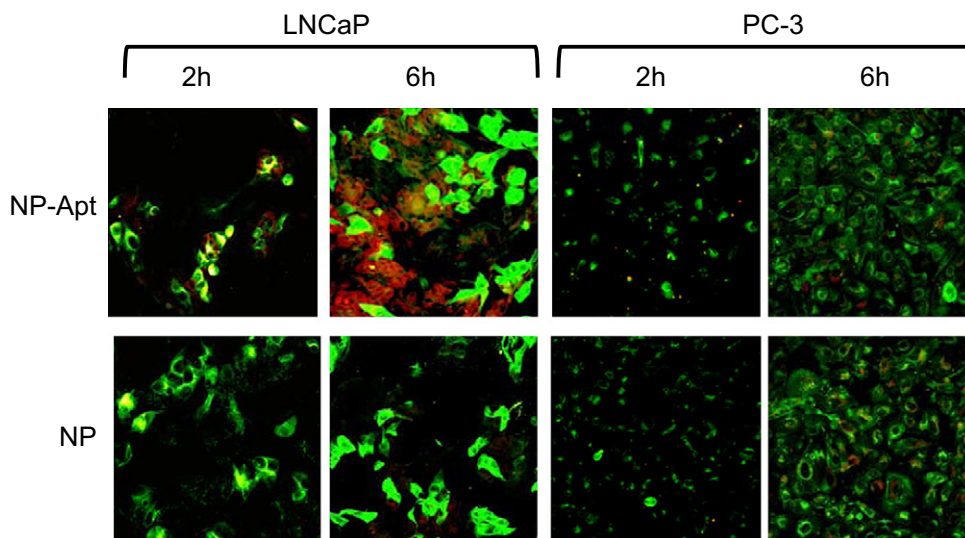
**Fig. 12.** Confocal images of LNCaP (left) and PC-3 (right) cells treated with aptamer-functionalized nanoparticles (NP–Apt, top) and nanoparticles without aptamer (NP, bottom). The Cy-5 incorporated NP or NP–Apt are shown in red colour. The cells counterstained with Alexa-Flour 488 Phalloidin (binding to cellular actin) are shown in green.

difference between the aptamer-Cy5 NC and the Cy5 NC without aptamer with respect to their capability of cell-binding and internalization. Incubating PC-3 cells with NCs for longer time resulted in slightly increased NC uptake. The binding of aptamer-Cy5 NCs to the PC-3 cells was substantially weaker than to LNCaP cells. These *in vitro* studies demonstrated that NCs conjugated with aptamer targeting ligand can potentially be used for prostate cancer targeting.

We have previously demonstrated that NCs can be formulated into solid form when albumin is used as the lyoprotectant. We next tested whether aptamer-Cy5 NCs can be made in solid form and then reconstituted to give NCs with similar sizes and targeting capability. At a BSA/aptamer-Cy5 NC mass ratio of 10, the size of the lyophilized and reconstituted aptmaer-Cy5 NC was 212.6 nm (with a polydispersity of 0.386) as compared to NCs with 157.1 nm (with a polydispersity of 0.144) before lyophilization. DLS analysis indicated that the lyophilized and reconstituted aptamer-Cy5 NCs maintain monomodal size distribution (data not shown). The reconstituted aptamer-Cy5 NCs were then applied in cell-binding studies and analyzed by FACS; their targeting capability was found to be well preserved during the lyophilization process.

## 4. Conclusion

In summary, we developed various techniques that allow for formulation of polymeric nanoconjugates with controlled chemophysical and biological properties. We developed a one step, co-precipitation method to formulate nanoconjugates that could stay non-aggregated in a salt solution with the use amphiphilic triblock copolymer as the surfactant for particle surface modification. We also discovered that albumin can function as an excellent lyoprotectant and successfully achieved the solid formulation of nanoconjugates that could be reconstituted with absolutely no particle aggregation. By incorporating the albumin-based lyoprotection technique, we demonstrated for the first time that polymer nanoparticles containing a conjugated nucleic acid targeting ligand can be prepared in solid form that can be reconstituted to well-dispersed, non-aggregated particles and well-maintained targeting capability. These new formulation strategies and findings can potentially be broadly employed for the controlled preparation of numerous other polymeric nanomedicines for basic sciences as well as for clinical applications.

## Appendix

Figures with essential colour discrimination. Certain figures in this article, in particular Figs. 1, 2, 11 and 12, may be difficult to interpret in black and white. The full colour images can be found in the on-line version, at doi:10.1016/j.biomaterials.2010.01.009.

## References

[1] Tong R, Cheng JJ. Anticancer polymeric nanomedicines. Polym Rev 2007;47(3):345–81.
[2] Tong R, Christian DA, Tang L, Cabral H, Baker JR, Kataoka K, et al. Nanopolymeric therapeutics. MRS Bull 2009;34(6):422–31.
[3] Moghimi SM, Hunter AC, Murray JC. Nanomedicine: current status and future prospects. FASEB J 2005;19(3):311–30.
[4] Duncan R. Polymer conjugates as anticancer nanomedicines. Nat Rev Cancer 2006;6(9):688–701.
[5] Zhang L, Gu FX, Chan JM, Wang AZ, Langer RS, Farokhzad OC. Nanoparticles in medicine: therapeutic applications and developments. Clin Pharmacol Ther 2008;83(5):761–9.
[6] Avgoustakis K. Pegylated poly(lactide) and poly(lactide-*co*-glycolide) nanoparticles: preparation, properties and possible applications in drug delivery. Curr Drug Deliv 2004;1(4):321–33.
[7] Goodman TT, Olive PL, Pun SH. Increased nanoparticle penetration in collagenase-treated multicellullar spheroids. Int J Nanomedicine 2007;2(2):265–74.
[8] Alexis F, Pridgen E, Molnar LK, Farokhzad OC. Factors affecting the clearance and biodistribution of polymeric nanoparticles. Mol Pharm 2008;5(4):505–15.
[9] Tong R, Cheng JJ. Paclitaxel-initiated, controlled polymerization of lactide for the formulation of polymeric nanoparticulate delivery vehicles. Angew Chem Int Ed Engl 2008;47(26):4830–4.
[10] Tong R, Cheng JJ. Ring-opening polymerization-mediated controlled formulation of polylactide-drug nanoparticles. J Am Chem Soc 2009;131(13):4744–54.
[11] Dong Y, Feng SS. In vitro and in vivo evaluation of methoxy polyethylene glycol-polylactide (MPEG-PLA) nanoparticles for small-molecule drug chemotherapy. Biomaterials 2007;28(28):4154–60.

[12] Teply BA, Tong R, Jeong SY, Luther G, Sherifi I, Yim CH, et al. The use of charge-coupled polymeric microparticles and micromagnets for modulating the bioavailability of orally delivered macromolecules. Biomaterials 2008; 29(9):1216–23.

[13] Cheng JJ, Teply BA, Sherifi I, Sung J, Luther G, Gu FX, et al. Formulation of functionalized PLGA–PEG nanoparticles for in vivo targeted drug delivery. Biomaterials 2007;28(5):869–76.

[14] Musumeci T, Ventura CA, Giannone I, Ruozi B, Montenegro L, Pignatello R, et al. PLA/PLGA nanoparticles for sustained release of docetaxel. Int J Pharm 2006;325(1–2):172–9.

[15] Hamblett KJ, Senter PD, Chace DF, Sun MMC, Lenox J, Cerveny CG, et al. Effects of drug loading on the antitumor activity of a monoclonal antibody drug conjugate. Clin Cancer Res 2004;10(20):7063–70.

[16] Schluep T, Hwang J, Cheng JJ, Heidel JD, Bartlett DW, Hollister B, et al. Preclinical efficacy of the camptothecin-polymer conjugate IT-101 in multiple cancer models. Clin Cancer Res 2006;12(5):1606–14.

[17] Chamberlain BM, Cheng M, Moore DR, Ovitt TM, Lobkovsky EB, Coates GW. Polymerization of lactide with zinc and magnesium beta-diiminate complexes: stereocontrol and mechanism. J Am Chem Soc 2001;123(14):3229–38.

[18] O'Keefe BJ, Hillmyer MA, Tolman WB. Polymerization of lactide and related cyclic esters by discrete metal complexes. J Chem Soc Dalton Trans 2001;(15):: 2215–24.

[19] Cheng JJ, Deming TJ. Synthesis and conformational analysis of optically active poly(beta-peptides). Macromolecules 2001;34(15):5169–74.

[20] Lu H, Cheng JJ. N-trimethylsilyl amines for controlled ring-opening polymerization of amino acid N-carboxyanhydrides and facile end group functionalization of polypeptides. J Am Chem Soc 2008;130(38):12562–3.

[21] Ouchi M, Terashima T, Sawamoto M. Transition metal-catalyzed living radical polymerization: toward perfection in catalysis and precision polymer synthesis. Chem Rev 2009;109(11):4963–5050.

[22] Farokhzad OC, Cheng JJ, Teply BA, Sherifi I, Jon S, Kantoff PW, et al. Targeted nanoparticle–aptamer bioconjugates for cancer chemotherapy in vivo. Proc Natl Acad Sci U S A 2006;103(16):6315–20.

[23] Gref R, Minamitake Y, Peracchia MT, Trubetskoy V, Torchilin V, Langer R. Biodegradable long-circulating polymeric nanospheres. Science 1994; 263(5153):1600–3.

[24] Maeda H, Wu J, Sawa T, Matsumura Y, Hori K. Tumor vascular permeability and the EPR effect in macromolecular therapeutics: a review. J Control Release 2000;65(1–2):271–84.

[25] Bilati U, Allemann E, Doelker E. Development of a nanoprecipitation method intended for the entrapment of hydrophilic drugs into nanoparticles. Eur J Pharm Sci 2005;24(1):67–75.

[26] Galindo-Rodriguez S, Allemann E, Fessi H, Doelker E. Physicochemical parameters associated with nanoparticle formation in the salting-out, emulsification-diffusion, and nanoprecipitation methods. Pharm Res 2004;21(8):1428–39.

[27] Moghimi SM, Hunter AC, Murray JC. Long-circulating and target-specific nanoparticles: theory to practice. Pharmacol Rev 2001;53(2):283–318.

[28] Moghimi SM, Muir IS, Illum L, Davis SS, Kolbbachofen V. Coating particles with a plock-copolymer (Poloxamine-908) suppresses opsonization but permits the activity of dysopsonins in the serum. Biochim Biophys Acta 1993;1179(2):157–65.

[29] Roberts MJ, Bentley MD, Harris JM. Chemistry for peptide and protein PEGylation. Adv Drug Deliv Rev 2002;54(4):459–76.

[30] Schluep T, Cheng JJ, Khin KT, Davis ME. Pharmacokinetics and biodistribution of the camptothecin-polymer conjugate IT-101 in rats and tumor-bearing mice. Cancer Chemother Pharmacol 2006;57(5):654–62.

[31] Fukuda J, Khademhosseini A, Yeh J, Eng G, Cheng JJ, Farokhzad OC, et al. Micropatterned cell co-cultures using layer-by-layer deposition of extracellular matrix components. Biomaterials 2006;27(8):1479–86.

[32] Karp JM, Yeh J, Eng G, Fukuda J, Blumling J, Suh KY, et al. Controlling size, shape and homogeneity of embryoid bodies using poly(ethylene glycol) microwells. Lab Chip 2007;7(6):786–94.

[33] Kjoniksen AL, Joabsson F, Thuresson K, Nystrom B. Salt-induced aggregation of polystyrene latex particles in aqueous solutions of a hydrophobically modified nonionic cellulose derivative and its unmodified analogue. J Phys Chem B 1999;103(45):9818–25.

[34] Pun SH, Tack F, Bellocq NC, Cheng JJ, Grubbs BH, Jensen GS, et al. Targeted delivery of RNA-cleaving DNA enzyme (DNAzyme) to tumor tissue by transferrin-modified, cyclodextrin-based particles. Cancer Biol Ther 2004;3(7): 641–50.

[35] Dai ZL, Piao LH, Zhang XF, Deng MX, Chen XS, Jing XB. Probing the micellization of diblock and triblock copolymers of poly(L-lactide) and poly(ethylene glycol) in aqueous and NaCl salt solutions. Colloid Polymer Sci 2004;282(4): 343–50.

[36] Musumeci T, Vicari L, Ventura CA, Gulisano M, Pignatello R, Puglisi G. Lyoprotected nanosphere formulations for paclitaxel controlled delivery. J Nanosci Nanotechnol 2006;6(9–10):3118–25.

[37] Wagner V, Dullaart A, Bock AK, Zweck A. The emerging nanomedicine landscape. Nat Biotechnol 2006;24(10):1211–7.

[38] Tuerk C, Gold L. Systematic evolution of ligands by exponential enrichment–RNA ligands to bacteriophage-T4 DNA-polymerase. Science 1990;249(4968):505–10.

[39] Ellington AD, Szostak JW. In vitro selection of RNA molecules that bind specific ligands. Nature 1990;346(6287):818–22.

[40] Ellington AD, Szostak JW. Selection in vitro of single-stranded-DNA molecules that fold into specific ligand-binding structures. Nature 1992;355(6363): 850–2.

[41] Nimjee SM, Rusconi CP, Sullenger BA. Aptamers: an emerging class of therapeutics. Annu Rev Med 2005;56:555–6.

[42] Lupold SE, Hicke BJ, Lin Y, Coffey DS. Identification and characterization of nuclease-stabilized RNA molecules that bind human prostate cancer cells via the prostate-specific membrane antigen. Cancer Res 2002;62(14):4029–33.

[43] Farokhzad OC, Jon SY, Khadelmhosseini A, Tran TNT, LaVan DA, Langer R. Nanoparticle–aptamer bioconjugates: a new approach for targeting prostate cancer cells. Cancer Res 2004;64(21):7668–72.